Uptake of Gas-Phase Ammonia. 2. Uptake by Sulfuric Acid Surfaces

E. Swartz, Q. Shi, and P. Davidovits*

Department of Chemistry, Merkert Chemistry Center, Boston College, Chestnut Hill, Massachusetts 02167-3809

J. T. Jayne, D. R. Worsnop, and C. E. Kolb

Center for Aerosol and Cloud Chemistry, Aerodyne Research, Inc., Billerica, Massachusetts 01821-3976

Received: May 24, 1999; In Final Form: August 16, 1999

The uptake of gas-phase ammonia by sulfuric acid surfaces was measured as a function of temperature (248−288 K), gas−liquid interaction time (2−15 ms), and acid concentration (20−70 wt % H_2SO_4) using a droplet train apparatus. The uptake coefficient increases as a function of acid concentration and reaches unity at about 55 wt % H_2SO_4. The increased NH_3 uptake in acid solution is apparently due to reaction between NH_3 and H^+ at the gas−liquid interface. The results yielded parameters required to model the reaction of NH_3 with H^+ at the gas−liquid interface. These uptake experiments were expanded to include a detailed study of gas transport to a moving train of droplets. An analysis of previous sulfuric acid aerosol neutralization experiments shows that the uptake of ammonia by ternary $NH_3-H_2SO_4-H_2O$ solutions is significantly lower than that by fresh binary $H_2SO_4-H_2O$ solutions. At typical tropospheric water and ammonia vapor concentrations, NH_3 uptake coefficients need to be included in detailed microphysical models of sulfuric acid aerosols.

Introduction

Aerosols play an important role in the atmospheric chemistry of both the stratosphere and the troposphere. Aerosols also affect the earth's climate by directly scattering radiation, and indirectly, by serving as cloud condensation nuclei (CCN). The number of cloud droplets formed is directly proportional to the number density of cloud condensation nuclei. The size, density and composition of these cloud droplets in turn determine the effect of clouds on the Earth's albedo.[1]

Ammonium (NH_4^+) and sulfate (SO_4^{-2}) are two of the primary ionic components in cloud condensation nuclei. Ammonia (NH_3) in the atmosphere originates primarily from surface sources, including decaying organic matter and chemical fertilizers. Sources of sulfur in the atmosphere include biogenic species such as CH_3SCH_3, H_2S, OCS, anthropogenic sources (mostly SO_2), and volcanic emissions (principally SO_2). These emitted species are in the S(IV) oxidation state and are further oxidized in the atmosphere to form S(VI), principally H_2SO_4, which in turn plays a key role in the formation of aerosols.

Current models for tropospheric aerosol growth depend on the condensation rates of gaseous ammonia, sulfuric acid, and water vapor.[2] Because atmospheric water vapor levels are high, aerosol growth rates are largely governed by the uptake of H_2SO_4 and NH_3 vapors. Recent measurements have shown that the uptake coefficient for H_2SO_4 vapor is near unity (essentially collision limited).[3,4] Well determined values for the uptake coefficient for NH_3(g) by acidic aerosols are required for quantitative modeling of atmospheric aerosol growth rates.

Knowledge of the ammonia uptake rate is also important in view of a recent suggestion[5,6] that ternary nucleation of $NH_3-H_2SO_4-H_2O$ vapors is a likely explanation of fast new particle formation rates inferred from field measurements of ultrafine particles.[5,7−8] Modeling of such particle formation rates in the atmosphere depends critically on the competition between condensation on preexisting particles and new particle nucleation. New particle formation is favored by slow gas uptake rates on preexisting particles, which increase steady-state vapor levels.[9]

Previous studies of NH_3(g) interactions with H_2SO_4 liquid surfaces include a molecular beam scattering study [10−13] and several flow reactor aerosol neutralization experiments.[14−17] In the scattering study the absence of detectable inelastic scattering was interpreted as evidence for a unity uptake coefficient on concentrated H_2SO_4 solution (98.8 wt %). In the aerosol studies, ammonia−aerosol interaction times are mostly on the order of seconds. On the basis of composition changes observed in collected aerosols, NH_3(g) uptake coefficients ranging from 0.1 to 0.5 were deduced. In all these studies, the concentration of NH_3(g) was such that the composition of the aerosol was changing significantly during the experiment, making it difficult to extract kinetic parameters for binary sulfuric acid solutions.

In the present work we study the interaction of NH_3(g) with H_2SO_4/H_2O surfaces, using the droplet train apparatus. The gas-phase NH_3 density was low (5×10^{12} cm^{-3}), and the gas−liquid interaction time was on the order of milliseconds. The low gas-phase concentration of NH_3(g) and the short gas−liquid interaction time minimize droplet composition changes. The uptake of gas-phase ammonia by aqueous sulfuric acid was measured as a function gas−liquid interaction time (2−15 ms), acid concentration (20−70 wt % H_2SO_4), and temperature (248−288 K). The results yielded parameters required to model the reaction of NH_3 with H^+ at the gas−liquid interface.

A proper understanding of gas phase diffusive transport of the trace gas to the droplet train is central to an accurate analysis of our uptake data. In our previous gas uptake experiments with aqueous droplets, the flow tube pressure was relatively high set by the equilibrium water vapor pressure (4−20 Torr). This

10.1021/jp991697h CCC: $18.00
Published on Web 10/14/1999

limited the range of pressures over which we could test our understanding of gas-phase diffusion. By contrast, in the present studies with sulfuric acid droplets, the partial pressure of H_2O vapor is relatively low. For example, for a 70 wt % H_2SO_4 solution at 250 K, the equilibrium water vapor pressure is only 0.02 Torr. The overall pressure in the flow tube is then determined principally by the inert carrier gas. Under these conditions, it is possible to significantly expand our previous studies of trace gas uptake by a moving train of droplets and place our understanding of gas-phase diffusive transport on a firmer footing.

The apparatus, basic experimental procedure, data analysis and modeling used in this study are described in the preceding companion article.[18] Here, we will present only those aspects of the experiment, which are specific to the NH_3-sulfuric acid studies.

Experimental Section

Uptake measurements of NH_3(g) on sulfuric acid were performed using a droplet train apparatus similar to the one shown in Figure 2 of the preceding article.[18] The apparatus was modified to allow work with cold concentrated acid droplets as described by Robinson et al.[19] Gas uptake was measured by passing a fast-moving (1500−3000 cm/s) and monodisperse (50 to 350 μm in diameter) collimated train of aqueous acid droplets through a 30 cm long longitudinal low-pressure flow tube which contained trace amounts of NH_3 entrained in a flowing mixture of carrier (rare gas) and water vapor. Carrier gases are introduced at the entrance of the reactor. Trace gases (diluted in rare gas) are introduced through one of three loop injectors located along the flow tube. By selecting the injector and the droplet velocity, the gas−droplet interaction time can be varied between 2 and 15 ms.

Sulfuric acid solutions were prepared by diluting known volumes of reagent grade sulfuric acid (95−98 wt %) with known volumes of distilled water. The concentrations were determined from the densities of the solutions which were measured by weighing 10 mL aliquots. [20] The accuracy of these concentration measurements is about ±0.5 wt %.

The droplet stream was produced by forcing the acid solution through a platinum electron microscope aperture surrounded by a doughnut-shaped piezoelectric ceramic. Before flowing through the nozzle aperture, the acid solution was precooled using an external temperature controlled circulating bath. A chromel−alumel thermocouple in a stainless steel sheath was fixed in place just above the aperture and provided a continuous measure of the droplet stream temperature. As the droplets traverse the flow tube, they equilibrate with the ambient water vapor. To minimize evaporation, which would change droplet surface temperature and concentration, a flow of H_2O in helium matched to the water vapor pressure over the acid droplet was introduced into the droplet generation region of the flow tube. In previous experiments with this apparatus, direct measurements of water vapor densities demonstrated that droplet surface acid concentrations in the gas/droplet interaction region are within 0.5 wt % of their initial value and that the droplet temperature is known to within $\sim \pm 2$ °C.[21]

Gas uptake is determined by measuring the trace gas concentration (n_g) downstream of the flow tube as the surface area of the droplets is changed in a stepwise fashion, by varying the driving frequency of the piezoelectric ceramic. A measured decrease in the trace gas signal (Δn_g) resulting from an increase in the exposed droplet surface area corresponds to an uptake of the gas by the droplet surface. The uptake coefficient (γ_{meas}), as defined in Shi et al.,[18] was obtained from the measured change in trace gas signal via eq 1:

$$\gamma_{meas} = \frac{4F_g}{\bar{c}\Delta A} \ln \frac{n_g}{n_g'} \tag{1}$$

The parameters are defined as in Shi et al.,[18] F_g is the carrier-gas volume rate of flow (cm^3 s^{-1}) through the system, $\Delta A = A_1 - A_2$ is the change in the total droplet surface area in contact with the trace gas, and n_g and n_g' are the trace gas densities at the outlet of the flow tube after exposure to trains of droplets of area A_2 and A_1, respectively ($n_g = n_g' + \Delta n_g$).

The gases exiting the reaction zone flow through a multipass absorption cell (White cell) with an effective path length of about 750 cm. The NH_3 vapor is detected via tunable infrared diode laser differential absorption. The NH_3 absorption line used in these experiments is at a frequency of 965.3538 cm^{-1}, with a line strength of 4.32×10^{-19} cm^2 molecule^{-1} cm^{-1}.[22] Initial trace gas densities of $\sim 5 \times 10^{12}$ cm^{-3} (typical in these experiments) yield a fractional absorbance of ~10%.

Pressure differences between the flow tube and the droplet collection chamber were monitored and balanced. In other recent experiments[19,23] the pressure balance was checked further by monitoring the concentration of an inert reference gas, typically methane, which is added to the flow. The change in the density of the inert gas monitors the effect of the sweep-out and/or pressure unbalance as droplet frequency is changed. In the present ammonia study, absorption lines for an appropriate reference gas were not available with the diode laser. However, changes in methane concentration due to sweep-out or pressure unbalance observed in previous studies were less than 0.5%, whereas NH_3 concentration changes due to uptake were in the range of 7−70%, depending on the droplet composition and temperature.

Modeling NH_3(g) Gas−Liquid Interactions

In our droplet train experiments, a gas-phase species, in this case NH_3(g), interacts with liquid droplets and the disappearance of that species from the gas phase is monitored. The disappearance of the species is expressed in terms of a measured uptake coefficient, γ_{meas}, which is related to the experimentally observed flux (J) into a surface as

$$J = \frac{n_g \bar{c} \gamma_{meas}}{4} \tag{2}$$

As is discussed in the companion paper,[18] gas uptake is a function of several inter-related processes which may include gas-phase and liquid-phase diffusion, mass accommodation, Henry's law solubility, bulk phase, and surface reactivity. Therefore, the parameter γ_{meas} represents a convolution of these processes, and the experimental challenge is to separate the contributions of these processes to the overall gas uptake.[21,23,24] Following the discussion in the previous paper and references therein, it is convenient to express the overall uptake process in terms of a resistance formulation,

$$\frac{1}{\gamma_{meas}} = \frac{1}{\Gamma_{diff}} + \frac{1}{S} + \frac{1}{\Gamma_s + \dfrac{1}{\dfrac{S-\alpha}{S\alpha} + \dfrac{1}{\Gamma_b}}} \tag{3}$$

where Γ_{diff} represents the rate of gas diffusion; S is the surface adsorption coefficient, defined as the fraction of collisions that

results in thermal accommodation of the trace gas onto the surface; Γ_s represents the effect on the uptake of surface processes; α is the mass accommodation coefficient (the probability that a molecule enters the bulk liquid phase upon collision with the surface); and Γ_b represents the rate of dissolution and reaction (if any) of species within the bulk liquid. This formulation aids the deconvolution of the various processes that control the overall gas uptake rate. In what follows, we will briefly discuss the bulk phase terms (Γ_{diff} and Γ_b) and then we will focus on the interfacial model that accounts for mass accommodation (α) and surface reactivity (Γ_s). In particular, the formulation of surface reactivity within the gas liquid interface will serve as a key to understanding how NH_3 uptake varies in acid solutions. Surface reactions may cause the uptake coefficient to exceed the limitation normally set by the mass accommodation coefficient.

Gas-Phase Diffusion. As discussed in the companion paper and references therein,[18] gas-phase diffusive transport of a trace gas to droplets does not lend itself to a straightforward analytical solution. However, an empirical formulation of diffusive transport to a stationary droplet developed by Fuchs and Sutugin[25] has been shown to be in good agreement with measurements, see Widmann and Davis[26]. Using the Fuchs−Sutugin formulation, Hanson et al.[27] extracted an expression for Γ_{diff} as

$$\frac{1}{\Gamma_{diff}} = \frac{0.75 + 0.283K_n}{K_n(1 + K_n)} \tag{4}$$

Here, K_n is Knudsen numbers defined as $2\lambda/d_f$, where λ is mean free path and $\lambda = 3D_g/\bar{c}$; d_f is the effective diameter of droplets for the diffusive process. In our early experiments, it was shown that diffusive transport to the train of moving droplets, closely spaced (2−12 droplet diameters), is independent of droplet diameter but depends rather on the diameter of the droplet-forming orifice d. (See Worsnop et al.[24]) Worsnop et al.[24] experimentally established the relationship between d_f and d as $d_f = (1.9 \pm 0.1)d$.

It is possible to formulate plausibility arguments suggesting why diffusive transport to a train of moving droplets depends on the diameter of the droplet-forming orifice, rather than on the diameter of the droplets. However, a convincing analytical formulation explaining this observation has so far not been obtained. Work toward this goal is continuing.

As was stated earlier, because of the low H_2O vapor pressure of the sulfuric acid droplets, the $NH_3(g)$ uptake measurements facilitated the study of diffusive transport over a wide range of Knudsen numbers ($K_n = 0.05-4.5$) with uptake coefficients ranging from 0.06 to 1. These studies are described in the Appendix to this paper. The results confirmed the earlier findings that diffusive transport to the train of moving droplets is independent of droplet diameter, yielding a value of $d_f = (2.0(\pm 0.1)d$ where d is the orifice diameter. The studies showed that over the full range of Knudsen numbers, gas-phase diffusive transport is in accord with the formulation of Fuchs and Sutugin[25] as expressed by eq 4.

On the basis of these results, we define γ_o as the uptake coefficient in the limit of "zero pressure", i.e., in the absence of gas diffusion limitations,

$$\frac{1}{\gamma_{meas}} = \frac{1}{\Gamma_{diff}} + \frac{1}{\gamma_o} \tag{5}$$

Solubility and Reactivity in the Bulk Liquid. In this section we discuss the effect of Henry's law solubility and chemical reactions of the NH_3 in the acid solution. The principal equilibrium processes governing NH_3 solubility in acid solutions are

$$NH_3(g) \overset{H}{\rightleftharpoons} NH_3(aq) \tag{6}$$

$$NH_3(aq) + H^+(aq) \underset{k_r'}{\overset{k_f'}{\rightleftharpoons}} NH_4^+(aq)\ (K_b') \tag{7}$$

K_b' is the equilibrium constant for reaction 7, $K_b' = k_f'/k_r'$. The overall solubility of $NH_3(g)$ can be expressed as an effective Henry's law coefficient H^* (M atm^{-1}) given by the sum of physically dissolved $NH_3(aq)$ and protonated $NH_4^+(aq)$.

$$\{[NH_3(aq)] + [NH_4^+(aq)]\} = H^* p_{NH_3} = [NH_3(g)]\ RTH^* = [NH_3(g)]\ H\ (1 + K_b'\ [H^+]) \tag{8}$$

Here p_{NH_3} is the partial pressure of ammonia (atm), and R is the gas constant (atm M^{-1} K^{-1}).

In acid solutions (pH < 2), the H^+ concentration is so large that the protonation step in the equilibrium is shifted far toward NH_4^+, making H^* sufficiently large (>10^9 M/atm) so that on the millisecond time scale of the droplet train experiment reaction 7 is irreversible. In other words, in the droplet train experiments under highly acidic conditions, reevaporation of dissolved NH_3 can be neglected. Under those conditions, Γ_b is determined by the forward reaction rate in eq 7, which is expressed by the term Γ_{rxn}.[28]

$$\Gamma_b = \Gamma_{rxn} = \frac{4HRT}{\bar{c}}\sqrt{D_l k_1} \tag{9}$$

Here k_1 is the pseudo first-order reaction rate for the formation of NH_4^+ in eq 7, given by

$$k_1 = k_f'[H^+] \tag{10}$$

The rate constant k_f' in eq 10 is 4.3×10^{10} M^{-1} s^{-1} at 293 K.[29] With this value of k_f', Γ_b is larger than 8 for pH < 2. The $1/\Gamma_b$ term is negligible compared to $1/\alpha$, and therefore, Γ_b is not rate limiting for $NH_3(g)$ uptake in acid solutions for pH < 2.

Interfacial Processes. Processes occurring at the gas−liquid interface can be taken into account via the kinetic model described in the companion paper (eq 5 in Shi et al.;[18] also see Nathanson et al.,[30] and Hanson[31]):

$$n_g \underset{k_{des}}{\overset{k_{ads}}{\rightleftharpoons}} n_s \overset{k_{sol}}{\rightarrow} n_l \overset{k_{rxn}}{\rightarrow} \text{product} \qquad n_s \overset{k_{surf}}{\downarrow} \text{product} \tag{11}$$

Here the subscripts g, s, and l represent the gas, surface, and liquid state of the species. In eq 11, the reverse processes going from the bulk to the interface (i.e., reverse rates parallel to k_{sol} and k_{rxn}) are accounted for by Γ_b and, as was noted, can be neglected for NH_3 uptake into acid solutions. Interfacial processes are then formulated in terms of mass accommodation (depending on k_{sol} and k_{des}) and surface reaction (depending on k_{surf}). As was stated in the preceding paper,

$$1/\alpha = 1/S + k_{des}/Sk_{sol} \tag{12}$$

As in Shi et al.,[18] here also, the adsorption coefficient S is expected to be close to unity.[30,32] For simplicity, here we will assume $S = 1$. Thus, the mass accommodation coefficient α

depends on the ratio k_{sol}/k_{des}, constrained to a maximum probability of unity by the adsorption collision rate.

Further, if we assume that $\Gamma_b = \Gamma_{rxn} \gg 1$, as is the case for NH_3 uptake into acid solution

$$1/\gamma_o = 1 + 1/(\Gamma_s + k_{sol}/k_{des}) \quad (13)$$

Here, as before, Γ_s represents the effect on the uptake of surface processes.

The mass accommodation coefficient is expressible as[33,30]

$$\alpha/(1-\alpha) = k_{sol}/k_{des} = \exp(-\Delta H_{obs}/RT + \Delta S_{obs}/R) \quad (14)$$

In the companion paper,[18] it was shown that, in aqueous solutions, in the pH range 0−4, the NH_3(g) uptake was limited by mass accommodation, and with reference to eq 14, α for NH_3(g) is characterized by $\Delta H_{obs} = -9.02 \pm 0.8$ kcal/mol and $\Delta S_{obs} = -35.9 \pm 2.9$ cal/(mol K). This corresponds to a negative temperature dependence of α, with α varying from 0.35 to 0.08 between 260 and 290 K.

Surface Reactivity. In aqueous solution (pH > 0), NH_3(g) uptake is described by mass accommodation as in eqs 13 and 14, with no evidence of surface reaction.[18,34] In contrast, as will be shown in the next section, the rate of NH_3(g) uptake into sulfuric acid solutions (H_2SO_4 concentration >20 wt %) increases sharply with acidity and the measured uptake coefficient is larger than the mass accommodation coefficient (α) for aqueous solutions. This increase is most consistently explained by a surface reaction as characterized by Γ_s in eq 13. (See Discussion section.) This surface reaction is most likely an acid catalyzed formation of NH_4^+ analogous to the bulk phase reaction in eq 7. That is,

$$NH_3(s) + H^+(s) \xrightarrow{k_{s2}} NH_4^+(s) \quad (15)$$

where the protonation of NH_3 occurs within the interface without species uptake into the bulk solution.

Surface reaction channels within the gas−liquid interface have been observed for a number of aqueous and acid systems. These include the reaction of $ClONO_2$ with HCl in H_2SO_4−H_2O solution,[35,36] reactions of halogen molecules with aqueous halide ions (e.g. Cl_2, $Br_2 + Br^-$, I^-),[37] $ClNO_2 + I^-$ reaction in aqueous solution,[38] and, most recently, acid and base-catalyzed D/H isotope exchange for deuterated ethanol on aqueous solutions.[39] The distinguishing feature of these studies is the observation that uptake rates are linearly proportional to reactant concentration, as opposed to the square root dependence for liquid diffusion-limited bulk reactivity (eq 9). In all these cases it was possible to distinguish between surface and bulk liquid reaction channels by performing a detailed analysis of uptake kinetics.

The effect of surface reactions on trace gas uptake is formulated in terms of n_s and k_{surf} in eq 11 and as derived in Shi et al.[18] (their eq 12), the surface uptake coefficient Γ_s is

$$\Gamma_s^{rxn} = \frac{4}{\bar{c}}(n_s/n_g)k_{surf} \quad (16)$$

Formally, n_g (cm^{-3}) and n_s (cm^{-2}) are the gas-phase and surface concentrations of ammonia and k_{surf} is the pseudo-first-order rate constant for the reaction of the interfacial ammonia with the H^+ ion.

A quantitative calculation of Γ_s requires knowledge of the magnitudes of these interfacial parameters. However, since these parameters are not known, they have to be estimated. We will assume that the interfacial parameters are linearly proportional to their bulk phase counterparts. In this approximation, we take the vapor−liquid interface to be a sharp but finite transition, a few molecular diameters thick, within which the molecular density increases from the gas to the liquid. We will assume that the thickness δ of the interface is 10^{-7} cm (10 Å).

The bulk-liquid-phase concentration n_l of ammonia can be expressed in terms of the gas-phase concentration, Henry's law coefficient (H) for ammonia and f_{NH_3}, the activity coefficient of NH_3 in acidic solutions. In accord with our assumption that the interfacial parameters are linearly proportional to their bulk phase counterparts, the ratio (n_s/n_g) can be expressed as

$$n_s/n_g = c_1 f_{NH_3} HRT\delta \quad (17)$$

where c_1 is an assumed constant of proportionality between the interfacial and bulk-liquid-phase ammonia concentrations.

In terms of the bulk phase parameters, the rate constant k_{surf} is

$$k_{surf} = c_2 a_{H^+} k_f' \quad (18)$$

Here a_{H^+} is the bulk concentration (or activity) of H^+, c_2 is the constant of proportionality between the interfacial and bulk H^+ concentrations, and k_f' is the rate for the NH_3(aq) reaction with H^+ in the bulk phase. (See eq 7.)

The activity coefficient of NH_3 in acidic solutions is not known. Therefore, we will approximate it with the activity of water a_{H_2O}. (See Hanson.[36]) The activity of water is a dimensionless parameter, defined as unity in pure water, which decreases with increased acidity.[40,41] With these assumptions, the surface uptake coefficient $\Gamma_s = \Gamma_s^{rxn}$ for ammonia is expressed as

$$\Gamma_s^{rxn} = 4\, c_1\, a_{H_2O}\, HRT\, [c_2\, a_{H^+}]\, k_f'\delta/\bar{c} \quad (19)$$

The Henry's law coefficient is obtained from the fitted values obtained in Shi et al.[18] Convenient representations of a_{H_2O} and a_{H^+} can be obtained from Tabazadeh et al.[42] and Michelsen,[43] respectively. These in turn provide analytical expressions for the exact formulation of Carslaw et al.[41] The rate coefficient k_f' is a diffusion-limited rate (see eq 10), and therefore, its temperature dependence will be inferred from the temperature dependence of the diffusion coefficient.[29]

Note that, in the formulation of eq 19, the dependence of Γ_s on reactant concentration (or activity, a_{H^+}) is linear. By contrast the bulk phase reactive uptake coefficient (Γ_{rxn}, in eq 9) depends on the square root of reactant concentration. With the assumptions stated above, the surface kinetics in eq 19 is characterized by the constants of proportionality c_1 and c_2. The experimental uptake data will provide the product c_1c_2.

Results and Analysis

Uptake Measurements. As an example of NH_3 uptake data, we show in Figure 1a and b plots of $\ln(n_g/n_g')$ as a function of $\bar{c}\Delta A/4F_g$ at 250 K and 70 wt % H_2SO_4. Here $\bar{c}\Delta A/4F_g$ was varied by changing the gas flow rate and the effective droplet surface area (ΔA). Each point in the figure is the average of at least 10 area change cycles with the error bars representing one standard deviation from the mean in the experimental $\Delta n_g/n_g$ value. In this experiment, the water pressure was set to 0.02 Torr, corresponding to the equilibrium H_2O vapor pressure of a 70 wt % H_2SO_4 solution at 250 K. The measurements shown in Figure 1a and b were performed under the same conditions except for the carrier gas pressure. The pressures in the experiments of Figure 1a and b were 4 Torr of He ($K_n = 1$)

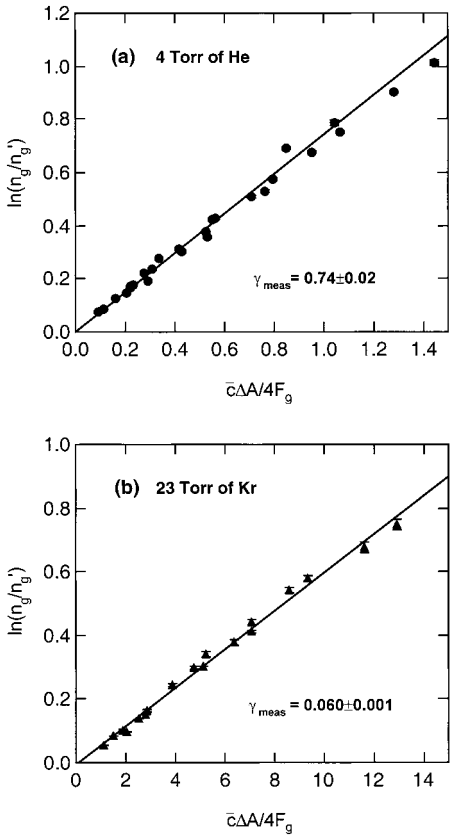

Figure 1. Plot of $\ln(n_g/n_{g'})$ versus $\bar{c}\Delta A/4F_g$ for NH_3(g) on 70 wt % H_2SO_4: $T = 250$ K, water vapor pressure = 0.02 Torr. (a) Carrier gas of 4 Torr He ($K_n = 1$), $\gamma_{meas} = 0.74 \pm 0.02$. (b) Carrier gas of 23 Torr Kr ($K_n = 0.05$), $\gamma_{meas} = 0.06 \pm 0.001$. Both measurements correspond to $\gamma_o \sim 1$, after accounting for gas diffusion via eq 5.

and 23 Torr Kr ($K_n = 0.05$), respectively. (Note the abscissa scale differs in the two figures.) The higher pressure experiments were part of the gas-phase diffusive transport studies. The slopes of the lines in Figure 1a and b yield values for γ_{meas} of 0.74 ± 0.02 and 0.060 ± 0.001, respectively.

Data plots similar to these shown in Figure 1 were obtained for the full range of uptake studies. In these studies the uptake signal $\Delta n_g/n_g$ typically varied from 7% to 70%. The linearity of these plots over an order of magnitude validates the measurement procedure, indicating that the uptake is well described by a single value of γ_{meas}, as in eq 1. The difference in uptake rates for the two plots in Figure 1 is due to the effect of gas-phase diffusion (Γ_{diff}), which is much slower in 23 Torr of Kr than that in 4 Torr He. In fact, using eqs 4 and 5, it is evident that the γ_{meas} values in both Figure 1a and b correspond to $\gamma_o = 1$ for NH_3(g) uptake into 70 wt % H_2SO_4. (See Appendix.)

Uptake as a Function of Gas−Liquid Interaction Time. In Figure 2 we show the measured uptake coefficient γ_{meas} as a function of gas−liquid contact time for 20, 40, and 70 wt % H_2SO_4 at 285 K. As is evident, no time dependence is observed in this data set. This is in accord with expectations since for sulfuric acid concentrations >20 wt %, the effective solubility is large ($H^* = 1.8 \times 10^{11}$ M atm^{-1} for 20 wt % H_2SO_4) and therefore $\Gamma_b \gg 1$. On the millisecond time scale of our experiments, the uptake is limited by α and Γ_s as described by eq 13.

In the sections that follow, uptake will be expressed in terms of γ_o after correcting γ_{meas} for gas-phase diffusion via eqs 4 and 5. For the results in Figure 2, γ_{meas} values of 0.24, 0.50,

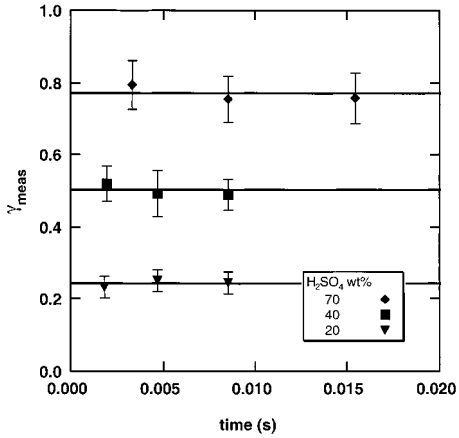

Figure 2. Uptake coefficient γ_{meas} as a function of gas−liquid contact time for NH_3(g) on 70 wt % H_2SO_4 (upper curve), 40 wt % H_2SO_4 (middle curve), and 20 wt % H_2SO_4 (lower curve) at $T = 285$ K.

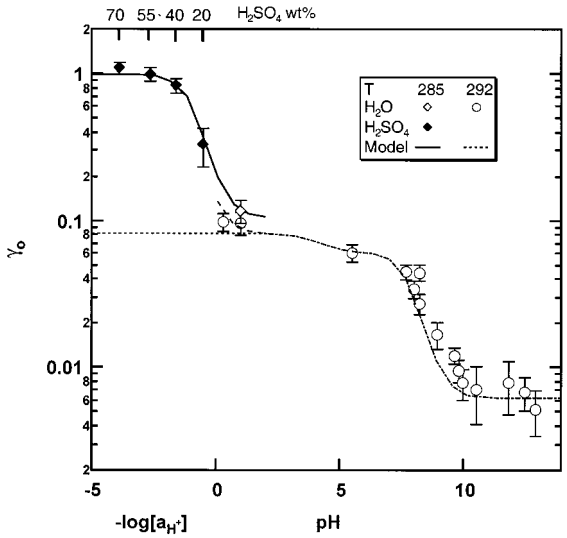

Figure 3. The uptake coefficient γ_o for NH_3 as a function of −log-[a_{H^+}]. The solid line is the plot of eq 13 with parameters as given in the text. Uptake results of Shi et al. (ref 18) on aqueous solution are shown as open symbols.

and 0.77 for 20, 40, and 70 wt % H_2SO_4 correspond to γ_o values of 0.34, 0.82, and 1.01, respectively.

Uptake as a Function of Acidity. In Figure 3, γ_o is plotted as a function of acidity. This is a specific set of data obtained at 285 K (closed diamonds). The solid line is a plot of eq 13 with $\alpha = 0.11$ as determined by Shi et al. (see eq 14).[18] In calculating Γ_s (eq 19), the value of c_1c_2 is (5.4 ± 2.0) × 10^{-4} obtained via a global fit to uptake data at all temperatures studied. (See next section.) For completeness, the plot includes experimental results on aqueous droplets obtained by Shi et al. at a slightly higher temperature of 291 K (open symbols) and at a gas−liquid contact time of 5 ms.[18] Acidity is defined as −log[a_{H^+}], where a_{H^+} is the activity of H^+. For aqueous solutions, [a_{H^+}] = [H^+] and acidity is equivalent to pH. In sulfuric acid solutions, the activity of H^+ is calculated using the multicomponent mole-fraction-based thermodynamic model of Carslaw et al.[41]

As discussed in Shi et al., the decrease in the uptake rate for pH > 4 is due to limitation imposed by NH_3 physical solubility (eq 6).[18] In this pH range the formation rate of NH_4^+ is reduced due to low H^+ concentration (eq 7). The plateau in the NH_3 uptake rate approached at pH < 4 in aqueous solution, is due to limitation imposed by the mass accommodation coefficient.

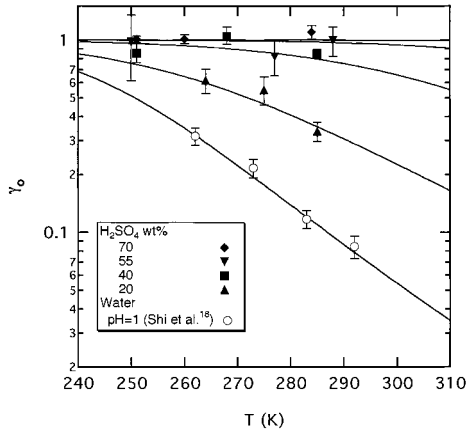

Figure 4. The uptake coefficient γ_o for NH_3 as a function of temperature. Solid points are from this study. Lines are the plots of eq 13 with α obtained by Shi et al. (ref 18). Best fit to the data yields $c_1c_2 = (5.4 \pm 2.0) \times 10^{-4}$ (see eq 19). Mass accommodation coefficients for NH_3 on aqueous solution at pH = 1, measured by Shi et al. (ref 18), are also shown (open circles).

In this region, Γ_b is much larger than α, Γ_s is negligible, and therefore here $\gamma_o = \alpha$ (eq 3 and 5). As will be shown, the increase in γ_o, beyond α in concentrated H_2SO_4 solution, can be explained by a surface reactivity.

Uptake as a Function of Temperature. In Figure 4, we show a plot of the uptake coefficients γ_o as a function of temperature for 20, 40, 55, and 70 wt % sulfuric acid. The figure, which is on a logarithmic scale, also shows the mass accommodation coefficients for NH_3 on aqueous solution at pH = 1 measured by Shi et al. as open circles.[18] (See Figure 6 in Shi et al.[18]). The negative temperature dependence of α is consistent with previous results.[18,33] It is important to note that with increasing H_2SO_4 concentration the magnitude of γ_o increases and the temperature dependence of γ_o decreases. The uptake coefficient γ_o reaches the limit of 1 for H_2SO_4 >50 wt %, at which point γ_o is independent of temperature.

The lines in Figures 3 and 4 connecting the experimental points are plots of eq 13 including the value of α measured by Shi et al. [18] and the surface NH_3 and H^+ reaction channel calculated via eq 19. The best fit to the data is obtained with the value of the product c_1c_2 in eq 19 equal to $(5.4 \pm 2.0) \times 10^{-4}$ (see eqs 17 and 18). This single value of c_1c_2 was used to fit the data at all temperatures.

Discussion

Interactions at the Gas−Liquid Interface. Figures 3 and 4 contain the principal findings of this study. In Figure 3, ammonia uptake is presented as a function of acid concentration from 70 wt % sulfuric acid to pH 13 ($-\log[a_{H^+}] = -4.0$ to 13, respectively). The present work together with that of Shi et al.[18] is the first presentation of the NH_3(g) uptake over a range of 17 orders of magnitude in H^+ activity.

As was noted in the preceding paper, the uptake coefficient above pH 10 is limited by the physical solubility of NH_3.[18] With increasing acidity, the solubility increases, and the uptake coefficient rises toward a plateau at about pH 2, where $\gamma_o = \alpha$, as discussed in Shi et al.[18] Perhaps the most notable feature in Figure 3 is the further rise of γ_o at higher acid concentrations, with γ_o reaching unity at ∼50 wt % H_2SO_4.

One might guess that the increase in γ_o for higher acid concentrations (> 10 wt % H_2SO_4) is due to an increase in the mass accommodation coefficient. However, two observations argue against this explanation. First, the uptake coefficient (γ_o) exhibits a plateau between pH = 0 and 3, suggesting that the increase below pH = 0 signals the onset of a new process. Second, in the uptake experiments with HCl(g) on sulfuric acid,[19] where no such increase in uptake with acidity was observed, the mass accommodation coefficient was shown to be independent of sulfuric acid concentration. We suggest that the increase in NH_3 uptake with acidity for pH < 0 is indicative of a separate process, most likely a surface specific reaction of NH_3 with H^+ ions near the gas−liquid interface.

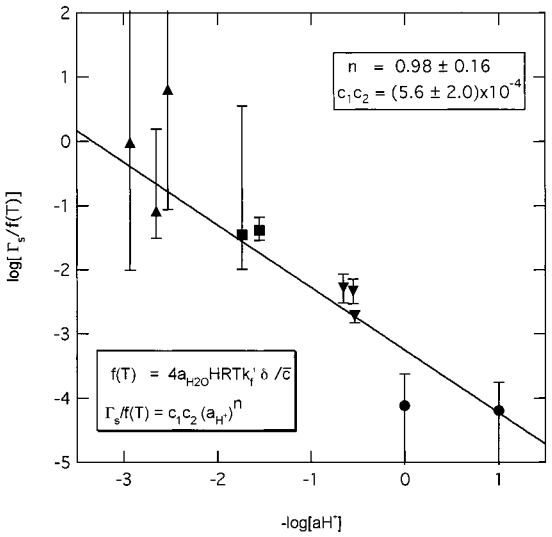

Figure 5. Dependence of Γ_s on a_{H^+}. Values of Γ_s derived from γ_o via eq 13 are adjusted as shown to facilitate display of data at all temperatures studied. The straight line is the best fit to the function $\Gamma_s = f(T)c_1c_2(a_{H^+})^n$; $f(T) = 4a_{H_2O}RTk_f'\delta/\bar{c}$. Solid line gives best-fit c_1c_2 and a_{H^+} power law as labeled.

The hypotheses of a surface specific reaction is supported by the observation that, in the region of increasing uptake (pH 0−55 wt % H_2SO_4), the rising part of the uptake coefficient γ_o is best fitted by a function Γ_s linear in a_{H^+} as formulated in eq 19. This is illustrated in Figure 5. Here we have extracted Γ_s values from experimental data via eq 13, and rearranged those values via eq 19 so that data obtained at different temperatures could be displayed on the same plot.[44] This entailed dividing Γ_s by the factor $f(T) = 4a_{H_2O}HRTk_f'\delta/\bar{c}$ and plotting the resulting expression as a function of a_{H^+} in logarithm space. Data are shown for the five temperatures studied. Error bars are calculated from uncertainties in Figure 4 using eq 13. The straight line is the best fit to the function $\Gamma_s = f(T)c_1c_2(a_{H^+})^n$. This procedure yields $n = 0.98 \pm 0.16$ and $c_1c_2 = (5.6 \pm 2.0) \times 10^{-4}$, which is in near exact agreement with the previously determined value $c_1c_2 = (5.4 \pm 2.0) \times 10^{-4}$. A dependence proportional to the square root of activity ($a_{H^+}^{1/2}$) consistent with bulk phase reaction does not fit the data. Clearly, the plot confirms the linear dependence of Γ_s on a_{H^+}, in accord with the hypotheses of a NH_3-H^+ surface reaction.

The factors c_1 and c_2 relate surface to bulk liquid values for solvated ammonia and H^+ (eqs 17 and 18). The small magnitude of c_1c_2, of order 5×10^{-4}, is not surprising. The interfacial density of H^+ is expected to be much lower than that in the bulk. Both calculations and experiments show that there is a substantial barrier for ions to approach the surface of an aqueous medium. In an experiment using laser induced second harmonic generation, Eisenthal estimated that an H^+ ion density at the surface is about two orders magnitude lower than in the bulk.[45] We do not have a reliable guide for estimating the surface density of ammonia. However, if c_2 were on the order 0.01 as suggested by the work of Eisenthal,[45] then c_1 (the ratio of surface

to bulk concentration of ammonia) would be about 0.056. This value obviously depends on several assumptions used in the formulation of eq 19, among them, for example, is the assumption that the physical solubility of NH_3 in acid solutions can be approximated by the activity of water, that is, by $f_{NH_3} \cong a_{H_2O}$.

Two conclusions can be drawn from Figure 5. First, the linear dependence on acid activity rather than on $a_{H^+}^{1/2}$ dependence provides the best fit to the experimental results. Second, the formulation of uptake that includes α and Γ_s as described in eqs 3, 15, and 19 accounts for the experimental observations including the plateau of $\gamma_o \sim 0.1$ in the pH region between 0 and 6.

Comparison with Previous Surface Studies. The results of three types of experiments can be usefully compared to the current work: gas uptake studies, beam studies, and aerosol neutralization studies.

Gas Uptake Studies. As was previously mentioned, a surface reaction channel at the gas−liquid interface was observed in several previous gas uptake studies.[35−39] In all these studies including the current one, two main factors identify surface reactions: (1) Enhancement of uptake over values that would be observed based on bulk phase processes and (2) a linear dependence of the enhancement on reactant concentration in the region of enhanced uptake. There is however, one notable difference between the previous and present surface reactivity studies. In the halogen/halide,[37] $ClNO_2 + I^-$ [38] and CH_3CH_2OD isotope exchange [39] studies, the uptake coefficient initially increased (linearly) as a function of reactant concentration and then reached a plateau at a value of the uptake coefficient (γ_o) less than unity. In those studies the plateau value of $\gamma_o < 1$ most likely reflects interfacial barriers between surface adsorbed species and solvated ions, similar to the free energy barrier inferred from negative temperature dependent α observations. (See discussion in Shi et al.[39]) By contrast, in the present NH_3(g) uptake study, $\gamma_o = 1$ at high acidities. This implies, that, even though the concentration of the H^+ ion at the interface is greatly reduced, the protonation of NH_3 is so highly favored (and the mobility of H^+ within the interface so large) that at high acidities, every ammonia molecule that strikes the surface irreversibly reacts to form NH_4^+. In this case there is no interfacial barrier to limit surface reactivity.

We note that uptake coefficients approaching unity have been observed in several other uptake studies on H_2SO_4 solutions both with and without indication of surface reactions. In the uptake of $ClONO_2$ + HCl on sulfuric acid, enhanced uptake due to surface reactivity was observed.[36] However the experiment was performed at low temperature (203 K), where α approaches unity, precluding separation of mass accommodation and surface reaction. Poschl et al. observed near unity uptake coefficients for gas-phase H_2SO_4 on liquid sulfuric acid, but this is most likely due to nearly unit mass accommodation probability.[4]

The uptake of HCl on H_2SO_4 solution is governed by the mass accommodation coefficient α, as indicated by a negative temperature dependence, with $\gamma_o < 1$ for $T > 240$ K, independent of sulfuric acid concentration.[19] There was no sign of surface reactivity. Even in concentrated acid solutions (40−50 wt %) HCl uptake is limited by mass accommodation (α), analogous to NH_3 (and CH_3CH_2OH) in aqueous solution.[18,39] It is evident that in both aqueous and acid solution, the uptake of HCl requires dissolution of the species, involving dissociation into H^+ and Cl^- ions. In contrast to ammonia that forms NH_4^+ at the interface, the dissociation of HCl, requiring solvation of both H^+ and Cl^-, does not occur at the interfacial region.

Beam Studies. The research group of Nathanson[11−13] conducted molecular beam scattering experiments of gases, including NH_3,[10] from films of highly concentrated H_2SO_4/H_2O solution (98.8 wt %). In those studies, the time-of-flight yields information on the degree of desorption of thermally adsorbed ("trapped") molecules. Uptake coefficients can be inferred from the extent of thermal desorption. For concentrated acid films, only species with high acid/base reactivity had uptake coefficients approaching unity as indicated by the absence of thermal desorption of trapped species. This includes NH_3 uptake results on 98.8% H_2SO_4, which is in agreement with results from our present NH_3 studies for $H_2SO_4 > 55$ wt %. While the scattering experiments cannot directly distinguish surface and bulk reactivity, Fiehrer and Nathanson[13] and Klassen et al.[12] suggest that the absence of thermal desorption is likely due to fast reactions within the interface, much as inferred here for NH_3 uptake in concentrated acid solution. Near-unit collision efficiency was also observed for isotope exchange of deuterated water and formic acid on H_2SO_4 surfaces, indicative of fast proton exchange. The inference of $\gamma_o \sim 1$ for ethanol (as well as ammonia) uptake into concentrated acid is of particular interest. The uptake behavior of CH_3CH_2OH is analogous to that of NH_3 in which both have an uptake coefficient $\gamma_o < 1$ on aqueous solutions.[46,39] Fiehrer and Nathanson[13] and Klassen et al.[12] interpreted the $\gamma_o \sim 1$ for CH_3CH_2OH on H_2SO_4 in terms of its basicity in the highly concentrated acid solution, analogous to NH_3 (eq 15). Smaller γ_o values for other species correlate inversely with basicity. The uptake behavior of HCl observed by Robinson et al. can be understood from this perspective. The acidic nature of HCl impedes dissociation in a highly acidic medium and prevents surface reaction. In contrast, the basicity of NH_3 is so large that $\gamma_o \sim 1$ via protonation is observed even at H_2SO_4 concentrations as low as 55 wt %.

Aerosol Neutralization Studies. To our knowledge, the only previous studies to have investigated NH_3(g) uptake into concentrated sulfuric acid solutions were experiments where the neutralization of acidic aerosols was measured.[14−17,47] These aerosol experiments differ from the current droplet studies in that the entire volume of the submicron aerosol equilibrates with the gas phase during the uptake experiment. Since the magnitude of NH_3 uptake is measured by the degree of neutralization of the collected aerosol, the very nature of the experiment is such that the composition of the sulfuric acid aerosol changes during the experiment. In most cases the NH_4^+/SO_4^{-2} ratio increases up to about 1. This is in contrast to the droplet experiments where the NH_4^+/SO_4^{-2} ratios remains <0.01, because of the short gas−liquid exposure time and the relatively low NH_3(g) concentration (5×10^{12} cm^{-3}). Thus, the range of uptake coefficients measured in the aerosol experiments, (0.1−0.5) is most likely due to the changing aerosol composition as the H_2SO_4 solution is neutralized.

The aerosol experiments of Huntzicker et al.[15] utilized an atmospheric pressure aerosol flow tube coupled to a sulfate analyzer, with a movable aerosol injector that permitted variable aerosol exposure times. This experiment included NH_3 uptake measurements at relatively low H_2SO_4 neutralization. They reported uptake coefficients in the range of 0.1−0.4, based on a kinetic model that assumed a constant uptake coefficient, independent of exposure time and composition. Our reanalysis of their data indicates that the uptake rate changed with time. The rate decreased as the aerosol was neutralized. In fact, for the shortest exposure time (0.5 s), corresponding to small composition changes ($NH_4^+/SO_4^{-2} < 0.05$), the observed uptake rate matched the gas diffusion limit at one atmosphere. That is,

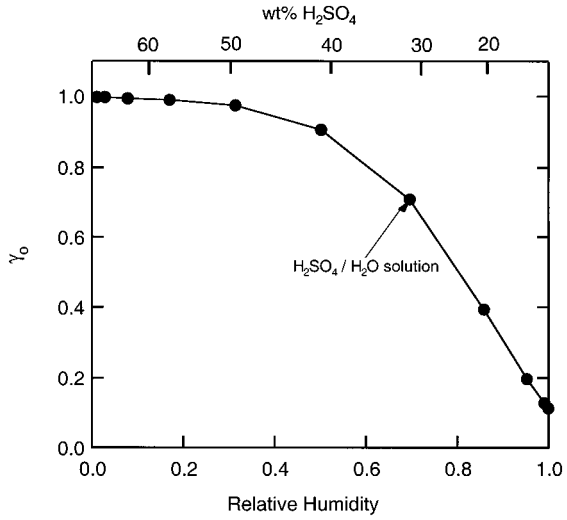

Figure 6. NH_3 uptake coefficient, γ_o, as a function of relative humidity at 290 K. Points are calculations obtained via eqs 13 and 19.

the measured uptake rate is consistent with $\gamma_o = 1$. For the experiments where detailed time dependent results were reported, reanalysis of the results indicates that $\gamma_o \leq 0.1$ as the NH_4^+/SO_4^{-2} ratio approaches 1.

The aerosol neutralization studies make it evident that the NH_3 content of the aerosol affects the NH_3(g) uptake rate. We attempted to model NH_3 uptake into $NH_3-H_2SO_4-H_2O$ ternary solution via eqs 13 and 19 using chemical activities (e.g., a_{H^+}) parametrized for the ternary solution by Clegg et al.[48] To fit the aerosol neutralization data, the product c_1c_2 in eq 19 has to be 5−10 times lower for NH_3 uptake into $NH_3-H_2SO_4-H_2O$ ternary solutions than that derived for the binary H_2SO_4/H_2O solution. This might reflect differences in NH_3 activity (i.e. physical solubility, represented by c_1) or the surface acidity (represented by c_2) in the binary and ternary solutions. Such differences might be expected since the added NH_3, forming ammonium sulfate, is likely to change the nature of the liquid, both bulk and surface.

Atmospheric Implications

As has been stated earlier, the concentration of H_2O vapor in the atmosphere far exceeds the concentrations of both NH_3 and H_2SO_4. Therefore, aerosol growth rates are relatively insensitive to the H_2O uptake coefficient and are governed primarily by the uptake coefficient of NH_3 and H_2SO_4. In Figure 6, we show the ammonia uptake coefficient (γ_o) at 290 K as a function of relative humidity (RH) obtained from Figures 3 and 4. These NH_3 uptake results, combined with recent measurements of H_2SO_4 accommodation coefficients,[4] indicate that on concentrated H_2SO_4 solution (RH < 30%) the uptake coefficients of both NH_3 and H_2SO_4 approach unity. Therefore, growth of concentrated H_2SO_4 aerosol is collision limited. However, the present results show that NH_3 uptake coefficients will be less than unity in the troposphere, where relative humidity is typically 30−40%, corresponding to H_2SO_4 compositions of 40−50 wt %.

The aerosol neutralization studies indicate that for the NH_4^+/SO_4^{-2} ratios larger than ~0.1, NH_3(g) uptake coefficients are likely to be less than unity even at low relative humidity (RH). Taken together, the dependence of the uptake coefficient on relative humidity presented here for binary $H_2SO_4-H_2O$ solutions and the reanalysis of NH_3 neutralization results imply that, under tropospheric conditions, with either high RH (≥40−60%) or high NH_3 content ($NH_4^+/SO_4^{-2} \geq 0.1-2$), NH_3 uptake coefficients will be less than unity, often as low as 0.1.

The magnitude of the gas uptake coefficient can indirectly affect aerosol nucleation in the atmosphere.[9,49] Nucleation of new aerosol particles is favored by slower uptake rates, since nucleation competes with condensation growth of preexisting aerosols. Slower uptake on preexisting particles results in higher steady-state levels of condensable vapor. This in turn increases the nucleation rate, which is a steep function of condensable species concentration.

If, as suggested by Weber et al.,[5] $NH_3-H_2SO_4-H_2O$ ternary nucleation is important in the atmosphere, then the relative humidity dependence of NH_3(g) uptake rates measured here and neutralization dependence as suggested by the aerosol experiments will be critical to microphysical modeling of steady-state levels of NH_3(g) in the atmosphere. Detailed modeling of atmospheric aerosol microphysics will require extension of the current NH_3(g) uptake study on binary $H_2SO_4-H_2O$ liquid solution to the ternary $NH_3-H_2SO_4-H_2O$ systems.

Finally, the question must be raised about the applicability of uptake coefficients obtained on macroscopic surfaces to uptake on ultrafine aerosol particles. The latter are defined as particles of diameter <100 nm, for which the surface tension and the equilibrium vapor pressure are significantly increased. It is not known how these perturbations affect the uptake rates. Specifically, uptake rates onto critical clusters, containing on the order of tens of molecules, might be significantly different, affecting new particle nucleation rates. Full understanding of gas/surface kinetics underlying aerosol microphysics, including aerosol nucleation and growth, will require extension of the gas uptake measurements to ultra-fine aerosol particles.

Acknowledgment. The authors thank Dr. Janice Cheung for extensive discussions. The authors acknowledge the $NH_3-H_2SO_4-H_2O$ model of Simon Clegg at http://www.uea.ac.uk/%7Ee770/aim.html. Funding for this work was provided by National Science Foundation Grants ATM-93-10407 and ATM-96-32599, the U.S. Environmental Protection Agency Grant R-821256-01-0, and Department of Energy Grants DE-FG02-91ER61208 and DE-FG02-94ER61854.

Appendix

Gas-Phase Diffusive Transport. As noted in the text, and discussed in the companion paper,[18] gas phase transport to a train of moving closely spaced droplets is well described by the Fuchs and Sutugin formulation (eq 4). However, as stated in the text, the transport rate does not depend on the droplet diameter but rather depends on the diameter of the droplet forming orifice.[24]

In the present uptake experiments on concentrated H_2SO_4 solutions, the H_2O vapor pressure is low and therefore gas phase diffusion rates are determined principally by the pressure of the inert carrier gas. As a result, gas-phase diffusive transport to the droplet train can be studied over a wide range of Knudsen numbers. To confirm and better quantify our understanding of gas diffusive transport, experiments were performed with several inert carrier gases (He, Ne, Ar, Kr) over a range of K_n from 0.05 to 4.5.

The gas transport coefficient in eq 4 is formulated in terms of the Knudsen number, $K_n = 2\lambda/d_f$, where d_f is the effective droplet diameter and λ is the mean free path, defined as $\lambda = 3D_g/\bar{c}$. The gas-phase diffusion coefficient D_g for NH_3(g) in a mixed carrier gas is calculated by[24]

$$\frac{1}{D_g} = \frac{p_{H_2O}}{D_{NH_3-H_2O}} + \frac{p_X}{D_{NH_3-X}} \qquad \text{(A-1)}$$

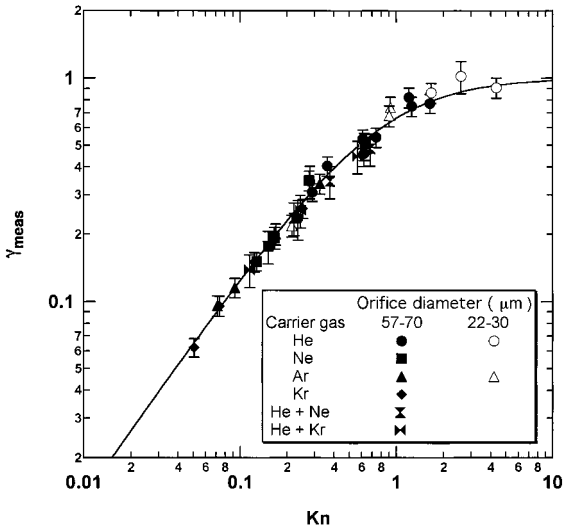

Figure 7. Plot of γ_{meas} as function of Knudsen number (K_n) for NH_3(g) uptake on 70 wt % H_2SO_4 droplets at 250, 263, and 284 K. Knudsen number is varied by changing the diameter of the droplet-forming orifice and by varying the carrier gas composition and pressure. (See inset.) Solid line is best fit to eq 3 with $\gamma_o = 1.02 \pm 0.04$.

Here, P_{H_2O} and P_X are the partial pressures (atm) of the water vapor and an inert carrier gas (X) in the flow tube, and $D_{NH_3-H_2O}$ and D_{NH_3-X} are the binary diffusion coefficients for NH_3(g) with water vapor and the inert gas, respectively. The values for binary gas-phase diffusion coefficients used in eq A-1 were calculated using CHEMKIN.[50] The program uses the following input parameters for NH_3(g): Lennard-Jones potential well depth ($\epsilon/k_B = 481.0$ K), Lennard-Jones collision diameter ($\sigma = 2.920$ Å), dipole moment ($\mu = 1.470$ D), and rotational relaxation collision number ($Z_{rot} = 10.00$).

In units of atm cm^2 s^{-1}, at 298 K, the calculated binary diffusion coefficients are $D_{NH_3-H_2O} = 0.215$, $D_{NH_3-He} = 0.901$, $D_{NH_3-Ne} = 0.417$, $D_{NH_3-Ar} = 0.233$, $D_{NH_3-Kr} = 0.184$. The diffusion coefficients with rare gases vary approximately as $T^{1.7}$, while $D_{NH_3-H_2O}$ varies as $T^{2.0}$.

Figure 1a and b illustrate the nature of gas-phase diffusion studies. Here the NH_3(g) uptake, in the form $\ln(n_g/n_g')$ is plotted as a function of $\bar{c}\Delta A/4F_g$, for 70 wt % H_2SO_4 at 250 K. The results shown in Figure 1a and b were obtained with carrier gases 4 Torr He and 23 Torr Kr, respectively. The other conditions of the experiment were identical. The slopes of the solid lines in the figure yield measured uptake coefficients $\gamma_{meas} = 0.74$ at 4 Torr He, and $\gamma_{meas} = 0.06$ at 23 Torr of Kr. Both values extrapolate, via eq 4, to $\gamma_o = 1$.

In Figure 7 we plot the uptake coefficients γ_{meas} as a function of the Knudsen number, for NH_3(g) obtained on 70 wt % H_2SO_4 at 250, 263, and 284 K. Each point on the curve was derived from plots such as shown in Figure 1. The Knudsen number was varied by changing the carrier gas (He, Ne, Ar, Kr) and its pressure in the range 3−24 Torr. The Knudsen number range was further extended by varying the orifice diameter. Orifices of several diameters were used. For simplicity of display, we will group them into two categories: 22−30 μm (open symbols) and 57−70 μm (closed symbols). In a given experiment, the diameter of the orifice was determined from liquid flow rate and droplet velocity measurements.[51] The solid line in Figure 7 is the best fit to the Fuchs and Sutugin[25] equation (eqs 4 and 5) yielding $\gamma_o = 1.02 \pm 0.04$. The diffusive process is independent of droplet diameter with the best fit obtained at $d_f = 2.0(\pm 0.1)d_o$, where d_o is the orifice diameter. This is in good agreement with the earlier result of Worsnop et al.[24] Such Fuchs and Sutugin plots (γ_{meas} vs K_n) were obtained for all the temperatures and sulfuric acid concentrations studied, confirming our treatment of gas-phase diffusion for γ_o in the range 0.3 to 1. Previous studies demonstrated the validity of our gas transport calculation at lower values of γ_o. As noted in the text, uptake rates were then reported as γ_o values obtained from γ_{meas} values via eqs 4 and 5.

Figure 7 demonstrates the applicability of the Fuchs and Sutugin formulation to the droplet train for a wide range of Knudsen numbers, gas mixtures, and uptake coefficients up to $\gamma_o = 1$. The data confirm that gas-phase diffusive transport to a stream of fast moving droplets can be formulated in terms of an effective diameter which depends not on the diameter of the droplet but rather on the diameter of the droplet-generating orifice.

References and Notes

(1) Finlayson-Pitts, B. J.; Pitts, J. N. *Atmospheric Chemistry*, John Wiley and Sons: New York, 1986.
(2) Kerminen, V. M.; Wexler, A. S.; Potukuchi, S., *J. Geophys. Res.* **1997**, *102*, 3715.
(3) Jefferson, A.; Eisele, F. L.; Ziemann, P. J.; Weber, R. J.; Marti, J. J.; McMurry, P. H. *J. Geophys. Res.* **1997**, *102*, 19, 021.
(4) Poschl, U.; Canagaratna, M.; Jayne, J. T.; Molina, L. T.; Kolb, C. E.; Molina, M. J. *J. Phys. Chem.* **1998**, *102*, 10082.
(5) Weber, R. J.; Marti, J. J. McMurry, P. H.; Eisele, F. L.; Tanner, D. J.; Jefferson, A. *Chem. Eng. Commun.* **1996**, *151*, 53.
(6) Coffman, D. J.; Hegg, D. A. *J. Geophys. Res.* **1995**, *100*, 7147.
(7) Weber, R. J.; McMurry, P. H.; Eisele, F. L.; Tanner, D. J. *J. Atmos. Sci.* **1995**, *52*, 2242.
(8) Weber, R. J.; Marti, J. J. McMurry, P. H.; Eisele, F. L.; Tanner, D. J.; Jefferson, A. *J. Geophys. Res.* **1997**, *102*, 4375.
(9) Russell, L. M.; Pandis S. N.; Seinfeld, J. H. *J. Geophys. Res.* **1994**, *99*, 20, 989.
(10) Fiehrer, K. M.; Nathanson, G. M. 1999. Private communication.
(11) Klassen, J. K.; Nathanson, G. M. *Science* **1996**, *273*, 333.
(12) Klassen, J. K.; Fiehrer, K. M.; Nathanson, G. M. *J. Phys. Chem. B* **1997**, *101*, 9098.
(13) Fiehrer, K. M.; Nathanson, G. M. *J. Am. Chem. Soc.* **1997**, *119*, 251.
(14) Robbins R. C.; Cadle, R. D. *J. Phys. Chem.* **1958**, *62*, 469.
(15) Huntzicker, J. J.; Cary, R. A.; Ling, Chaur-Sun *Environ. Sci. Technol.* **1980**, *14*, 819.
(16) McMurry, P. H.; Takano, H.; Anderson, G. R. *Environ. Sci. Technol.* **1983**, *17*, 347.
(17) Däumer, B.; Niessner, R.; Klockow, D. *J. Aerosol Sci*. **1992**, *23*, 315.
(18) Shi, Q.; Davidovits. P.; Worsnop, D. R.; Jayne, J. T.; Kolb, C. E. *J. Phys. Chem.* **1999**, *103*, 8812.
(19) Robinson, G. R.; Worsnop, D. R.; Jayne, J. T.; Kolb, C. E.; Swartz, E.; Davidovits. P. *J. Geophys. Res. [Atmos.]* **1998**, *103*, 25371.
(20) Perry, J. H. *Chemical Engineers Handbook*; McGraw-Hill: New York, 1950; pp 184 and 540.
(21) Robinson, G. R.; Worsnop, D. R.; Jayne, J. T.; Kolb, C. E.; Davidovits, P. *J. Geophys. Res. [Atmos.]* **1997**, *102*, 3583.
(22) Rothman, L. S.; Rinsland, C. P.; Goldman, A.; Massie, S. T.; Edward, D. P.; Flaud, J.-M.; Perrin, A.; Camy-Peyret, C.; Dana, V.; Mandin, J.-Y.; Schroeder, J.; Mccann, A.; Gamache, R. R.; Wattson, R. B.; Yoshino, K.; Chance, K. V.; Jucks, K. W.; Brown, L. R.; Nemtchinov, V.; Varanasi, P. *J. Quant. Spectrosc. Radiat. Transfer* **1998**, 665.
(23) Jayne, J. T.; Worsnop, D. R.; Kolb, C. E., Swartz, E.; Davidovits, P. *J. Phys. Chem.* **1996**, *100*, 8015.
(24) Worsnop, D. R.; Zahniser, M. S.; Kolb, C. E.; Gardner, J. A.; Watson, L. R.; Van Doren, J. M.; Jayne, J. T.; Davidovits, P. *J. Phys. Chem.* **1989**, *93*, 1159.
(25) Fuchs, N. A.; Sutugin, A. G. *Highly Dispersed Aerosols*; Ann Arbor Science Publishers: Ann Arbor, 1970.
(26) Widmann, J. F.; Davis, E. J. *J. Aerosol Sci.* **1997**, *28*, 87.
(27) Hanson, D. R.; Ravishankara, A. R.; Lovejoy, E. R. *J. Geophys. Res.* **1996**, *101*, 9063.
(28) Danckwerts, P. V. *Gas−Liquid Reactions*; McGraw-Hill: New York, 1970.
(29) Emerson, M. T.; Ernest, G.; Kromhout, R. A. *J. Chem. Phys.* **1960**, *33*, 547.
(30) Nathanson, G. M.; Davidovits, P.; Worsnop, D. R.; Kolb, C. E. *J. Phys. Chem.* **1996**, *100*, 13007.
(31) Hanson, D. R. *J. Phys. Chem.* **1997**, *101*, 4998.

(32) Mozurkewich, M.; McMurry, P. H.; Gupta, A.; Calvert, J. G. *J. Geophys. Res.* **1986**, *91*, 4163.
(33) Davidovits, P.; Jayne, J. T.; Duan, S. X.; Worsnop, D. R.; Zahniser, M. S.; Kolb, C. E. *J. Phys. Chem.* **1991**, *95*, 6337.
(34) The formation of a surface complex in the work of Shi et al. (ref 18) is, in this context, not regarded as a surface reaction.
(35) Hanson, D. R.; Ravishankara, A. R. *J. Phys. Chem*. **1994**, *98*, 5728.
(36) Hanson, D. R., *J. Phys. Chem.* **1998**, *102*, 4794.
(37) Hu, J. H.; Shi, Q.; Davidovits, P.; Worsnop, D. R.; Zahniser, M. S., Kolb, C. E. *J. Phys. Chem*. **1995**, *99*, 8768.
(38) George, Ch.; Behnke, W.; Scheer, V.; Zetsch, C.; Magi, L.; Ponche, J. L.; Mirabel, Ph. *Geophy. Res. Lett*. **1994**, *22*, 1505.
(39) Shi, Q.; Li, Y. Q.; Davidovits, P.; Worsnop, D. R.; Jayne, J. T.; Kolb, C. E. *J. Phys. Chem*. **1999**, *103*, 2417.
(40) Pitzer K. S. *Activity Coefficients in Electrolyte Solutions, 2nd ed.;* CRC Press: Boca Raton, FL, 1991.
(41) Carslaw, K. S.; Clegg, S. L.; Brimblecombe, P. *J. Chem. Phys.* **1995**, *99*, 11, 557.
(42) Tabazadeh, A.; Toon, O. B.; Clegg, S. L.; Hamill, P. *Geophys. Res. Lett*. **1997**, *24*, 1931.
(43) Michelsen, H. A. *Geophys. Res. Lett.* **1998**, *25*, 3571.
(44) Only data up to 55 wt % H_2SO_4 were used, since past this point γ_o approaches unity and further increase in Γ_s does not substantially affect the uptake.
(45) Eisenthal, K. B. *Acc. Chem. Res.* **1993**, *26*, 636.
(46) Jayne, J. T.; Duan, S. X.; Davidovits, P.; Worsnop, D. R.; Zahniser, M. S.; Kolb, C. E. *J. Phys. Chem*. **1991**, *95*, 6329.
(47) Rubel, G. O.; Gentry, J. W. *J. Aerosol Sci.* **1984**, *15*, 661.
(48) Clegg, S. L., Brimblecombe, P.; Wexler, A. S. *J. Phys. Chem.* **1998**, *102*, 2A, 2137.
(49) Pandis S. N.; Russell, L. M.; Seinfeld, J. H. *J. Geophys. Res*. **1994**, *99*, 16, 945.
(50) Kee, R. J.; Miller, J. H.; Jefferson, T. H. *CHEMKIN: A Chemical Kinetics Code Package*; Sandia Laboratories: Albuquerque, NM, 1989.
(51) Swartz, E. Ph.D. Thesis, Chemistry Department, Boston College, 1998.